Available online at www.eccomasproceedia.org
Eccomas Proceedia COMPDYN (2023) 3668-3676

ECCOMAS
Proceedia

COMPDYN 2023
9th ECCOMAS Thematic Conference on
Computational Methods in Structural Dynamics and Earthquake Engineering
M. Papadrakakis, M. Fragiadakis (eds.)
Athens, Greece, 12-14 June 2023

EVOLUTION OF THE MODAL PARAMETERS DUE PROGRESSIVE DEGRADATION OF AN RC BEAM-COLUMN JOINT

Angelo Aloisio[1], **Amedeo Gregori**[1,*], **Lorenzo Bizzarri**[1], **Caterina D'Agostino**[1], **Riccardo Cirella**[1], **Rocco Alaggio**[1]

[1] Università degli Studi dell'Aquila, Civil Environmental and Architectural Engineering Department, via Giovanni Gronchi n.18, L'Aquila 67100, Italy
e-mail: {angelo.aloisio1,amedeo.gregori,riccardo.cirella,rocco.alaggio}@univaq.it

---

Abstract. *This paper presents an experimental characterization of the progressive damage in reinforced concrete beam-columns joints from ambient vibration tests. During the quasi-static cyclic tests on an RC joint, the authors estimated the modal parameters corresponding to different stages of joint degradation. The variation of the modal parameters has been correlated to damage indicators of concrete, thus providing an answer to a well-debated topic concerning this case study: Are ambient vibration measurements informative for damage assessment? Which is the sensitivity of the modal parameters to the increasing damage levels? This preliminary study aims to understand the feasibility of vibration-based damage assessment at a component level for concrete structures to understand the modal parameters' sensitivity to damage at a system level.*

Keywords: Instructions, Structural Dynamics, Earthquake Engineering, Proceedings.

ISSN:2623-3347
Peer-review under responsibility of the organizing committee of COMPDYN 2023.
doi: 10.7712/120123.10670.20801

1 INTRODUCTION

Operational and cost constraints make often unfeasible forced-vibration tests (e.g., shaker and impact/pull-back tests) in civil structures. Consequently, ambient vibration (AV) is often the sole alternative method for damage detection purposes. In this approach, operational modal analysis (OMA) or output-only system identification techniques are used with AV data recorded before and after the structure has potentially suffered damage. According to Astroza et al. [3], there are three main limitations and challenges related to the use of OMA for damage detection.

- The need for automatic operational modal analysis. The automatic procedure allows to distinguish between spurious and physical modes, This is the most research aspect which received more attention, since many methods have been proposed in the last twenty years [17, 19, 12, 21, 16, 22, 7, 1, 14, 6].
- The statistical variability of the identified modal properties needs to be adequately investigated and understood because sources different to damage can also induce variations in the dynamic characteristics of civil structures, for example, temperature, measurement noise level, change in the boundary conditions, wind speed, etc. (e.g., [16, 13, 15, 4, 24]), as well as the uncertainty of the parameter estimation method itself.
- Third, the availability of data recorded on real structures undergoing real damage and degradation processes has been extremely limited. Most of the full-scale tests have been conducted on in-situ bridge structures condemned for demolition, in which artificial damage (e.g., partial saw cuts in steel girders, partial cuts of post-tensioning tendons) was induced during the demolition process [11, 9, 23, 5]. However, the induced type of artificial damage is not representative of real damage caused by natural loads or ageing.

There are a few studies attempting to assess the modal parameters of reinforced concrete (RC) buildings at different states of damage (e.g., [14, 10, 8]). However, except for the study by [3], none of the existing test, programs recorded AV data continuously and therefore implemented an automatic system identification approach, based on the data data recorded on a real structure subjected to damage induced by a realistic source of dynamic excitation. In this paper, the authors estimate the modal parameters of an RC joint subjected to progressive damage from quasi-static tests. The analyses reveal the variation of the modal parameters at a component level approach, never done before for RC joints.

2 EXPERIMENTAL TEST

The tested specimen consists of a T-shaped RC joint [2]. It represents the cellular unit of an RC frame. Fig.1(a) shows the tested specimen, while Fig.1(b) displays the layout of the ambient vibration test using Force Balance Accelerometers.

The experimental investigation derives from the superposition of two tests typology. (i) Quasi-static tests of the RC frame, as displayed in Fig.2(a), that shows the loading point and the constraints of the RC frame. (ii) Ambient vibration tests corresponding to different damage levels, identified by the maximum displacement value attained during the quasi-static test. The authors considered seven damage levels corresponding to the displacement values in mm: 23.70, -28.27, -31.27, 40.75, -52.55, -150, 300. Six accelerometers have been positioned on the RC frame, as shown in Fig.2(a). The acquisition duration is approximately 10 minutes at a 200Hz sampling frequency.

(a) (b)

Figure 1: (a) Tested specimen and (b) Experimental layout

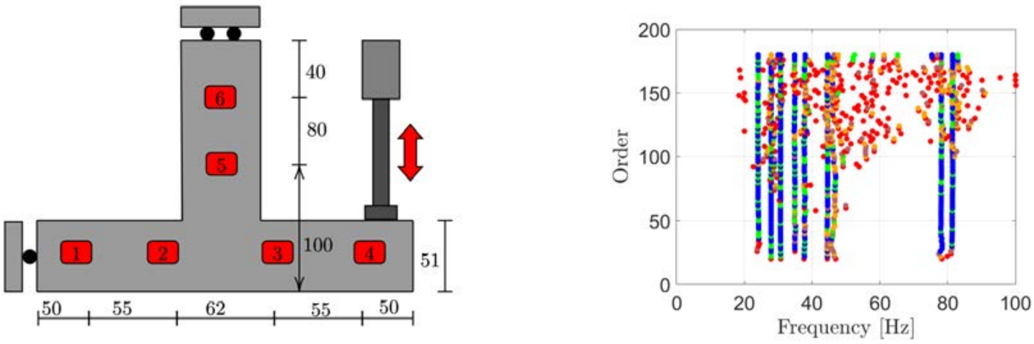

(a) (b)

Figure 2: (a) Experimental setup; (b) Stabilization diagram at the stage 0, no damage.

The data were processed using the SSI-cov algorithm [20], using the open-source software PyOMA [18]. Fig.2(b) shows the stabilization diagram obtained from the SSI-cov on the data corresponding to no damage. The dynamic identification provided a high-quality estimate of approximately seven modes in the range 0-100Hz.

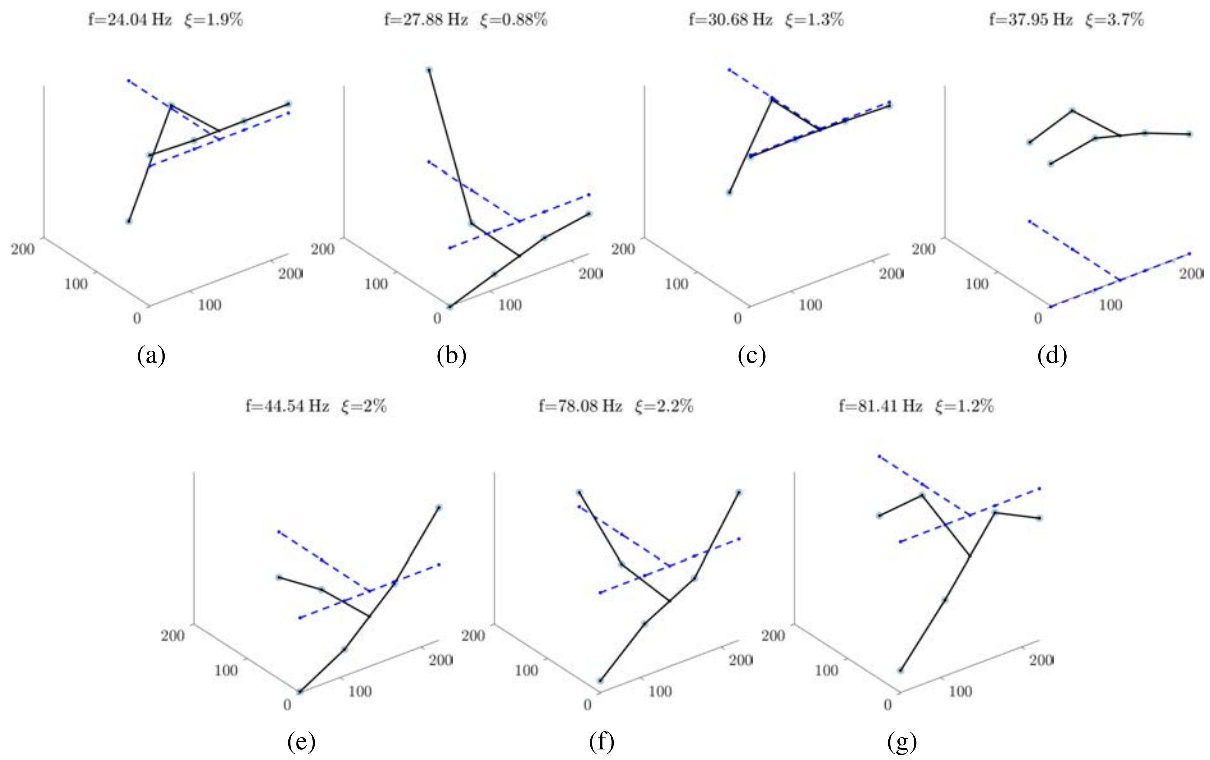

Figure 3: 3d representation of the experimental mode shapes corresponding to the undamaged phase.

Fig.3 shows a 3d representation of the experimental mode shapes corresponding to the undamaged phase. Additionally, Fig.4 shows a 2d representation of the experimental mode shapes corresponding to the undamaged phase. This representation helps us understand the in-plane distortion of the T-shaped element. The first mode at 24.04 Hz is characterized by more evident distortion at the joint. Therefore, its tracking might be the most informative approach to assess the effects of damages.

3 RESULTS AND DISCUSSION

Tab.1 resumes all the results of the dynamic identification for the eight considered stages. It collects the natural frequencies and damping values estimated in the undamaged phase (0) and the seven considered damage levels, labelled progressively from 1 to 7.

Tab.2 shows with a colour formating the Modal Assurance Distribution Matrices (MAC), obtained by comparing the modes estimated in two consecutive phases, namely states 0-1, 1-2, 2-3, 3-4, 4-5, 5-6, and 6-7.

The main aspects arising from the observation of the experimental data resumed in Tabs.1 and Tab.2 are:

- The progression of damage within the RC joint does not allow carrying out a modal tracking. The presence of damage significantly modifies the mode shape, as highlighted

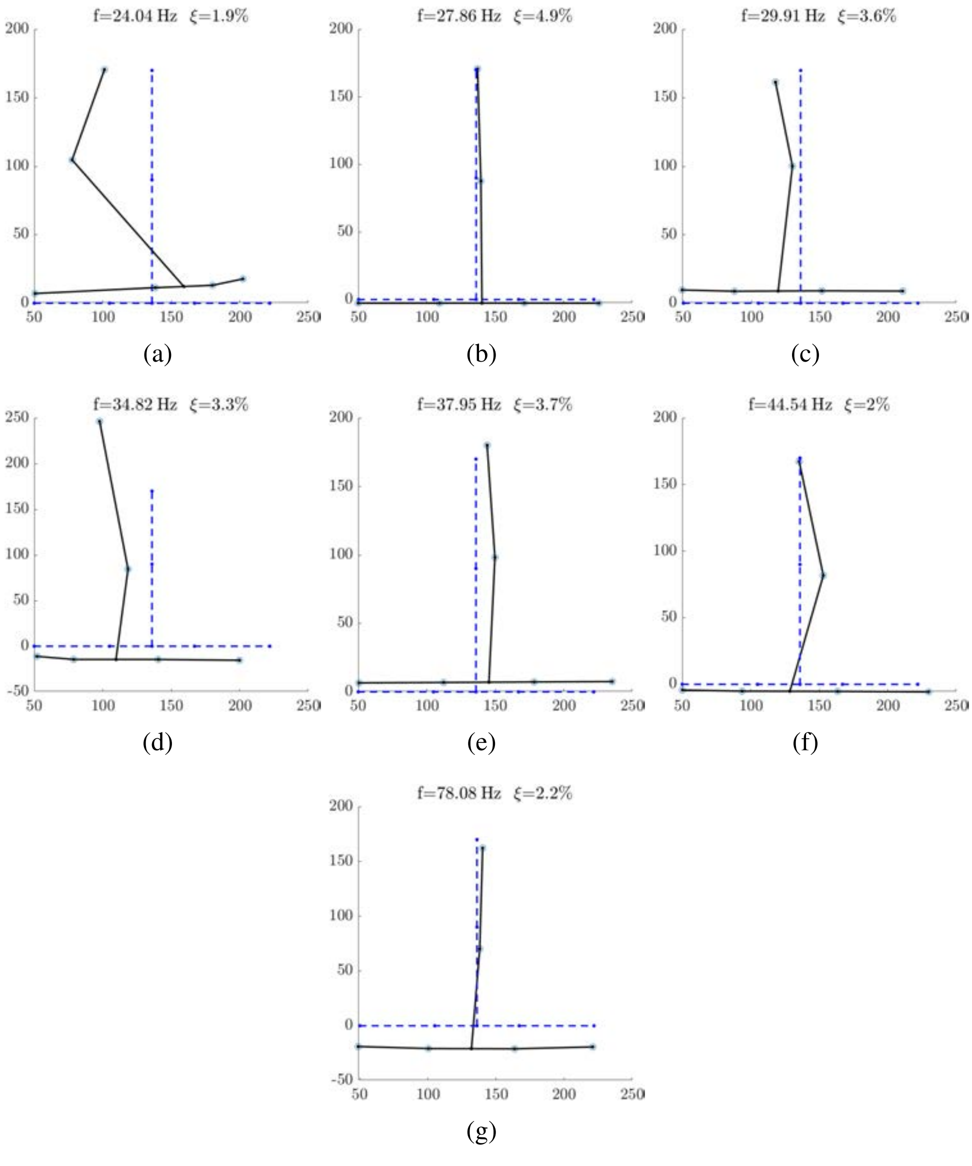

Figure 4: 2d representation of the experimental mode shapes corresponding to the undamaged phase.

Table 1: Natural frequencies and damping values estimated in the undamaged phase (0) and the seven considered damage levels.

	Damage level							
	0	1	2	3	4	5	6	7
f_1	24.04	24.52	24.03	24.21	23.74	20.71	18.51	12.67
f_2	27.86	33.04	32.59	33.40	33.43	31.29	19.61	26.07
f_3	29.91	37.30	37.38	38.60	39.25	39.86	32.74	32.35
f_4	34.82	48.44	49.21	42.26	42.20	49.34	40.00	33.32
f_5	37.95	52.15	50.25	50.12	50.10	50.60	42.59	39.18
f_6	44.54	53.29	52.68	51.99	52.26	55.35	52.27	46.00
f_7				54.96	55.28	63.57	55.20	49.06
f_8	78.08	65.99	65.58	65.21	65.39	79.81	64.89	75.01
f_9	81.41	86.98	83.53	82.17	80.19	85.07	81.15	84.24
ξ_1	1.85	0.60	1.54	0.88	1.17	1.29	2.38	0.50
ξ_2	4.92	1.70	4.55	0.99	1.31	3.09	2.18	0.89
ξ_3	3.60	3.46	2.96	3.86	0.61	1.61	1.29	0.62
ξ_4	3.26	3.63	1.39	4.79	4.39	2.16	2.63	2.69
ξ_5	3.72	1.48	3.92	1.36	1.32	2.22	2.44	2.45
ξ_6	2.02	1.10	1.55	1.33	2.26	1.89	0.40	1.21
ξ_7				0.82	1.16	1.28	1.10	2.08
ξ_8	2.17	2.23	1.77	1.74	1.99	0.93	1.49	2.02
ξ_9	1.21	1.41	1.77	2.73	1.08	4.12	2.09	1.64

Table 2: Representation of the MAC matrices. Each table shows the MAC computed between the modes of two consecutive states.

State 0

State 1	0.00	0.02	0.02	0.01	0.00	0.00	0.58	0.09
	0.13	0.77	0.70	0.01	0.50	0.04	0.02	0.00
	0.17	0.27	0.24	0.02	0.00	0.01	0.47	0.14
	0.08	0.47	0.45	0.00	0.38	0.02	0.00	0.10
	0.04	0.16	0.23	0.25	0.00	0.07	0.23	0.10
	0.58	0.04	0.06	0.71	0.05	0.78	0.14	0.41
	0.31	0.03	0.05	0.57	0.01	0.19	0.40	0.00
	0.08	0.02	0.03	0.25	0.00	0.01	0.45	0.08

State 1

State 2	0.00	0.02	0.02	0.01	0.00	0.00	0.58	0.09
	0.13	0.77	0.70	0.01	0.50	0.04	0.02	0.00
	0.17	0.27	0.24	0.02	0.00	0.01	0.47	0.14
	0.08	0.47	0.45	0.00	0.38	0.02	0.00	0.10
	0.04	0.16	0.23	0.25	0.00	0.07	0.23	0.10
	0.58	0.04	0.06	0.71	0.05	0.78	0.14	0.41
	0.31	0.03	0.05	0.57	0.01	0.19	0.40	0.00
	0.08	0.02	0.03	0.25	0.00	0.01	0.45	0.08

State 2

State 3	0.10	0.19	0.17	0.07	0.13	0.01	0.09	0.64
	0.28	0.00	0.00	0.99	0.47	0.01	0.02	0.03
	0.27	0.00	0.00	0.97	0.51	0.00	0.03	0.06
	0.00	0.00	0.14	0.04	0.00	0.03	0.10	0.98
	0.21	0.17	0.04	0.28	0.01	0.24	0.12	0.01
	0.02	0.08	0.18	0.00	0.08	0.04	0.01	0.78
	0.03	0.09	0.00	0.01	0.02	0.29	0.73	0.17
	0.14	0.15	0.09	0.03	0.55	0.30	0.02	0.05

State 3

State 4	0.64	0.39	0.69	0.46	0.08	0.00	0.12	0.34	0.21
	0.01	0.06	0.01	0.10	0.01	0.02	0.15	0.00	0.04
	0.00	0.00	0.00	0.05	0.02	0.02	0.02	0.02	0.00
	0.45	0.35	0.46	0.18	0.20	0.01	0.29	0.98	0.72
	0.21	0.11	0.20	0.21	0.11	0.06	0.34	0.58	0.72
	0.05	0.12	0.04	0.02	0.02	0.04	0.25	0.00	0.09
	0.09	0.21	0.03	0.06	0.38	0.00	0.00	0.01	0.10
	0.02	0.07	0.01	0.13	0.02	0.04	0.00	0.00	0.17

State 4

State 5	0.99	0.56	0.75	0.15	0.08	0.08	0.43	0.13	0.09
	0.90	0.45	0.81	0.17	0.13	0.23	0.30	0.31	0.22
	0.93	0.47	0.62	0.14	0.04	0.03	0.43	0.06	0.06
	0.26	0.26	0.08	0.01	0.01	0.11	0.21	0.10	0.10
	0.28	0.02	0.08	0.04	0.23	0.29	0.21	0.29	0.07
	0.01	0.26	0.07	0.00	0.00	0.00	0.01	0.01	0.08
	0.15	0.00	0.06	1.00	0.30	0.01	0.27	0.00	0.34
	0.42	0.04	0.10	0.29	0.13	0.00	0.95	0.02	0.00
	0.29	0.08	0.09	0.23	0.09	0.03	0.82	0.03	0.01

State 5

State 6	0.00	0.99	0.48	0.00	0.43	0.05	0.11	0.02	0.02
	0.03	0.60	0.59	0.22	0.03	0.00	0.00	0.00	0.00
	0.01	0.80	0.47	0.05	0.09	0.00	0.00	0.00	0.07
	0.00	0.14	0.02	0.00	0.27	0.00	0.20	0.22	0.01
	0.02	0.08	0.00	0.00	0.11	0.03	0.01	0.00	0.12
	0.00	0.08	0.00	0.00	0.00	0.18	0.06	0.00	0.02
	0.06	0.39	0.05	0.01	0.92	0.47	0.36	0.11	0.05
	0.00	0.13	0.01	0.01	0.02	0.16	0.04	0.01	0.07
	0.06	0.10	0.00	0.07	0.00	0.11	0.00	0.02	0.19

State 6

State 7	0.00	0.99	0.48	0.00	0.43	0.05	0.11	0.02	0.02
	0.03	0.60	0.59	0.22	0.03	0.00	0.00	0.00	0.00
	0.01	0.80	0.47	0.05	0.09	0.00	0.00	0.00	0.07
	0.00	0.14	0.02	0.00	0.27	0.00	0.20	0.22	0.01
	0.02	0.08	0.00	0.00	0.11	0.03	0.01	0.00	0.12
	0.00	0.08	0.00	0.00	0.00	0.18	0.06	0.00	0.02
	0.06	0.39	0.05	0.01	0.92	0.47	0.36	0.11	0.05
	0.00	0.13	0.01	0.01	0.02	0.16	0.04	0.01	0.07
	0.06	0.10	0.00	0.07	0.00	0.11	0.00	0.02	0.19

by the MAC values, which are generally very low, also when comparing mode shapes between two consecutive states of damage.

- The first modes are the ones characterized by the most evident decrement of the natural frequency. This is because the first mode is a distortion mode of the T-element, the one more affected by a stiffness reduction of the RC joint due to the presence of damage. The natural frequency reduces from almost 24.04 to approximately 12.67 Hz.
- Conversely, the higher modes are not characterized by a manifest in-plane deformation of the T- This is confirmed by the natural frequencies of the higher modes, which are almost independent of the damage phase. Paradoxically, the natural frequency of the last mode rises from 81 to 84 due to possible variations of the boundary conditions associated with the last damage phase.

4 CONCLUSIONS

This paper presents the results of an experimental campaign aiming at characterizing the effects of damage on an RC joint, tested quasi-statically in terms of modal parameters. The authors identified seven stages of the quasi-static test of the joint for carrying out seven ambient vibration tests. The supposed goal was to make a sort of modal tracking, i.e. following the evolution of the mode shape of the specimen as the damage progresses inside the node. However, the experimental tests highlighted two aspects. Only the modes associated with a significant distortion component manifest a frequency reduction associated with a stiffness loss in the RC joint. The second aspect relates to the difficulty in modal tracking. The mode shapes exhibit a significant variation between the different phases of damage. Accordingly, it is nearly impossible to state which mode became what since the modes modified substantially, yielding MAC values lower than 0.4, approximately. The frequency of the first distortion mode reduced from nearly 24 to 12 Hz. Future research efforts will assess the relationship between the frequency and stiffness loss of the joint through FE numerical modelling.

REFERENCES

[1] Rocco Alaggio, Angelo Aloisio, Elena Antonacci, and Riccardo Cirella. Two-years static and dynamic monitoring of the santa maria di collemaggio basilica. *Construction and Building Materials*, 268:121069, 2021.

[2] Michele Angiolilli, Amedeo Gregori, Roberto Tonelli, Claudio Tonelli, Edoardo Ciuffetelli, and Alfredo Peditto. Structural performance of unreinforced full-scale façade concrete beam-column joint under cyclic load. *Procedia Structural Integrity*, 44:870–877, 2023.

[3] Rodrigo Astroza, Hamed Ebrahimian, Joel P Conte, José I Restrepo, and Tara C Hutchinson. Statistical analysis of the modal properties of a seismically-damaged five-story rc building identified using ambient vibration data. *Journal of Building Engineering*, 52:104411, 2022.

[4] R. Ceravolo, G. Coletta, G. Miraglia, and F. Palma. Statistical correlation between environmental time series and data from long-term monitoring of buildings. *Mechanical Systems and Signal Processing*, 152, 2021. cited By 17.

[5] M. Dilena and A. Morassi. Dynamic testing of a damaged bridge. *Mechanical Systems and Signal Processing*, 25(5):1485–1507, 2011. cited By 84.

[6] M. Fraser, A. Elgamal, X. He, and J.P. Conte. Sensor network for structural health monitoring of a highway bridge. *Journal of Computing in Civil Engineering*, 24(1):11–24, 2010. cited By 95.

[7] C. Gentile, A. Ruccolo, and F. Canali. Continuous monitoring of the milan cathedral: dynamic characteristics and vibration-based shm. *Journal of Civil Structural Health Monitoring*, 9(5):671–688, 2019. cited By 20.

[8] H. Hien and A. Mita. Damage identification of full scale four-story steel building using multi-input multi-output models. volume 7981, 2011. cited By 4.

[9] O. Huth, G. Feltrin, J. Maeck, N. Kilic, and M. Motavalli. Damage identification using modal data: Experiences on a prestressed concrete bridge. *Journal of Structural Engineering*, 131(12):1898–1910, 2005. cited By 160.

[10] X. Ji, G.L. Fenves, K. Kajiwara, and M. Nakashima. Seismic damage detection of a full-scale shaking table test structure. *Journal of Structural Engineering*, 137(1):14–21, 2011. cited By 79.

[11] R.G. Lauzon and J.T. DeWolf. Ambient vibration monitoring of a highway bridge undergoing a destructive test. *Journal of Bridge Engineering*, 11(5):602–610, 2006. cited By 25.

[12] F. Magalhães, A. Cunha, and E. Caetano. Online automatic identification of the modal parameters of a long span arch bridge. *Mechanical Systems and Signal Processing*, 23(2):316–329, 2009. cited By 365.

[13] B. Moaveni, X. He, J.P. Conte, M. Fraser, and A. Elgamal. Uncertainty analysis of voigt bridge modal parameters due to changing environmental condition. *International Conference on Modal Analysis*, 2009. cited By 1.

[14] B. Moaveni, X. He, J.P. Conte, J.I. Restrepo, and M. Panagiotou. System identification study of a 7-story full-scale building slice tested on the ucsd-nees shake table. *Journal of Structural Engineering*, 137(6):705–717, 2011. cited By 115.

[15] R.D. Nayeri, S.F. Masri, R.G. Ghanem, and R.L. Nigbor. A novel approach for the structural identification and monitoring of a full-scale 17-story building based on ambient vibration measurements. *Smart Materials and Structures*, 17(2), 2008. cited By 145.

[16] C. Pan, X. Ye, and L. Mei. Improved automatic operational modal analysis method and application to large-scale bridges. *Journal of Bridge Engineering*, 26(8), 2021. cited By 6.

[17] R.S. Pappa, G.H. James III, and D.C. Zimmerman. Autonomous modal identification of the space shuttle tail rudder. *Journal of Spacecraft and Rockets*, 35(2):163–169, 1998. cited By 66.

[18] Dag Pasquale Pasca, Angelo Aloisio, Marco Martino Rosso, and Stefanos Sotiropoulos. Pyoma and pyoma_gui: A python module and software for operational modal analysis. *SoftwareX*, 20:101216, 2022.

[19] B. Peeters and G. De Roeck. One-year monitoring of the z24-bridge: Environmental effectsversus damage events. *Earthquake Engineering and Structural Dynamics*, 30(2):149–171, 2001. cited By 821.

[20] Bart Peeters and Guido De Roeck. Reference-based stochastic subspace identification for output-only modal analysis. *Mechanical systems and signal processing*, 13(6):855–878, 1999.

[21] C. Rainieri and G. Fabbrocino. Automated output-only dynamic identification of civil engineering structures. *Mechanical Systems and Signal Processing*, 24(3):678–695, 2010. cited By 161.

[22] E. Reynders, J. Houbrechts, and G. De Roeck. Fully automated (operational) modal analysis. *Mechanical Systems and Signal Processing*, 29:228–250, 2012. cited By 311.

[23] D.M. Siringoringo, Y. Fujino, and T. Nagayama. Dynamic characteristics of an overpass bridge in a full-scale destructive test. *Journal of Engineering Mechanics*, 139(6):691–701, 2013. cited By 27.

[24] F. Ubertini, G. Comanducci, N. Cavalagli, A. Laura Pisello, A. Luigi Materazzi, and F. Cotana. Environmental effects on natural frequencies of the san pietro bell tower in perugia, italy, and their removal for structural performance assessment. *Mechanical Systems and Signal Processing*, 82:307–322, 2017. cited By 135.